

# Experimental and Numerical Study on Heat Transfer Characteristics of Supercritical Carbon Dioxide Flowing Upward in a Vertical Tube

Jian Chen<sup>1</sup>, Rui Zhao<sup>1</sup>, Wen-Long Cheng<sup>1\*</sup>

1 Department of Thermal Science and Energy Engineering, University of Science and Technology of China, Hefei, Anhui 230027, PR China

## ABSTRACT

The supercritical carbon dioxide (S-CO<sub>2</sub>) Brayton cycle is widely applied in energy conversion systems, the heat transfer characteristics of S-CO<sub>2</sub> is an important factor affecting the cycle efficiency. The heat transfer characteristics of S-CO<sub>2</sub> flowing upward in a vertical tube ( $d=4.57\text{mm}$ ) is studied in this paper by experimental and numerical method. The numerical results are verified by experiments. And experiments are performed to analyze the parameter effects on heat transfer characteristics. The distributions of radial velocity and turbulent kinetic energy at different axial positions are obtained by numerical method to analyze the heat transfer mechanism. The results show that the effect of buoyancy flattens the velocity distribution, resulting in the weakening of turbulence intensity and the deterioration of heat transfer. Heat transfer deterioration occurs while  $q/G \geq 0.1\text{kJ/kg}$ . The heat transfer performance is better at higher mass flux or lower heat flux. Pressure and inlet temperature affect heat transfer only while the fluid state is near the pseudo-critical region. Based on the experimental data, a heat transfer correlation is proposed, the largest prediction deviation is less than 25%.

**Keywords:** heat transfer characteristics, supercritical CO<sub>2</sub>, flowing upward, buoyancy effect

## NONMENCLATURE

### Abbreviations

S-CO <sub>2</sub>	Supercritical CO <sub>2</sub>
htc	Heat transfer coefficient[W/(m <sup>2</sup> · K)]

### Symbols

$c_p$	Specific heat[J/(kg · K)]
$G$	Mass flux[kg/(m <sup>2</sup> · s)]
$h$	Enthalpy[kJ/kg]
$P$	Pressure[MPa]

$q$	Heat flux[kW/m <sup>2</sup> ]
$r$	Radial coordinate[m]
$R$	Tube radius[m]
$T$	Temperature[°C]
$\lambda$	Thermal conductivity[W/(m · K)]
$\rho$	Density[kg/m <sup>3</sup> ]
<i>Subscripts</i>	
b	Bulk
in	Inlet
out	Outlet
w	Wall

## 1. INTRODUCTION

Carbon dioxide is a kind of environmental protection natural working fluid which has been widely used in many engineering practices. Supercritical carbon dioxide Brayton cycle has been widely used in the field of energy conversion because of its high efficiency, compact structure and no pollution[1]. It has potential application in waste heat recovery system, geothermal system, solar energy system and other fields. The cycle efficiency is critical to energy conversion and utilization, the heat transfer characteristic of S-CO<sub>2</sub> is an important factor affecting the cycle efficiency[2]. Thus, it is significant to understand the heat transfer characteristics of S-CO<sub>2</sub>.

The research on the heat transfer characteristics of S-CO<sub>2</sub> at home and abroad mainly focuses on the flow in the tube and heat exchangers [3,4]. Many scholars have conducted experimental or numerical studies on the heat transfer characteristics of S-CO<sub>2</sub>. Existing research results indicated that heat transfer enhancement, normal heat transfer and heat transfer deterioration may occur while S-CO<sub>2</sub> flows in vertical tubes. Zhang[5] found that mass flux has a great influence on heat transfer characteristics, no heat transfer deterioration is observed even though the heat flux is high while the mass flux is very low. Lei [6] found that the heat flux has

a great influence on the heat transfer at low mass flux. S.Yildiz [7] found that the heat transfer is easier to deteriorate in large tube diameters, and the heat transfer performance of the small tube diameters is better. Zhang[8] numerically studied the differences in heat transfer characteristics of S-CO<sub>2</sub> flowing in horizontal, vertical and vertical helical tubes, the results show that the buoyancy effect is different in the three kinds of tubes. The heat transfer deterioration occurs in the vertical tube, while the heat transfer performance is better in the horizontal tube and helical tube. Guo[9] numerically studied the heat transfer characteristics of S-CO<sub>2</sub> flowing in a tube under heating conditions. The results show that the buoyancy effect improves the downward flow heat transfer performance, while deteriorates that for upward flow under heating conditions, and it is found that decreasing the tube diameter and heat flux can alleviate heat transfer deterioration.

To sum up, due to the drastic changes in the physical properties of S-CO<sub>2</sub>, the heat transfer characteristics of S-CO<sub>2</sub> are different under different tubes and working conditions. In this study, the heat transfer characteristics of S-CO<sub>2</sub> flowing upward in a vertical tube ( $d=4.57\text{mm}$ ) is studied by experimental and numerical method. Experiments are performed to analyze the parameter effects on heat transfer characteristics. The distributions of radial velocity and turbulent kinetic energy at different axial positions are obtained by numerical method to analyze the heat transfer mechanism. And a heat transfer correlation is proposed.

## 2. EXPERIMENTS AND NUMERICAL METHODS

### 2.1 Experiment platform and test section

Figure 1(a) shows the schematic of S-CO<sub>2</sub> flowing in tube test platform. CO<sub>2</sub> filled the low-pressure CO<sub>2</sub> tank and flowed into the compressor, which can compress it to 20MPa. The compressed high pressure CO<sub>2</sub> is divided into two parts, one is the test channel (Line1), after passing through the throttle valve, the pressure drops to the range required by the experiments. The water bath is used for controlling the inlet temperature. The other part is the branch (Line2) for regulating the mass flow. Finally, two parts of CO<sub>2</sub> will converge and flow to low-pressure tank, forming a cycle.

The schematic diagram of the test section is shown in figure 1(b). The test section is a vertical circular tube made of 316L stainless steel. The outer and inner diameters of the tube are 6.35mm and 4.57mm, respectively. The length of the heating section is

1000mm and there is a 200mm adiabatic section in front of the inlet for the full development of the fluid flow. 20 T-type thermocouples with uncertainty  $\pm 0.2^\circ\text{C}$  are set at 50mm intervals on the tube wall. Before the experiment, calibration is carried out under the conditions of  $0^\circ\text{C}$  and  $100^\circ\text{C}$ . The test section is wrapped with thermal insulation cottons to reduce heat loss and insulated flanges are provided at both ends to ensure electrical insulation.

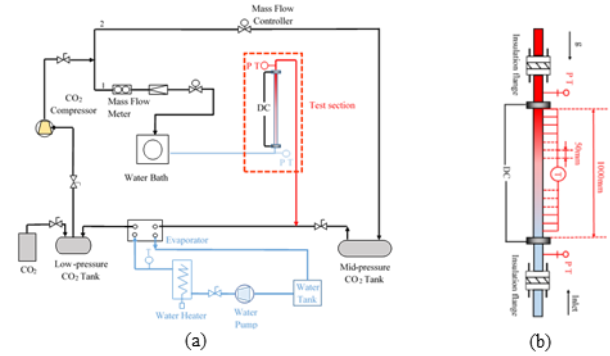


Fig. 1. (a)The schematic of S-CO<sub>2</sub> flowing in tube test platform  
(b)The schematic diagram of the test section

### 2.2 Data reduction

Because the wall thickness of the tube is small (0.89mm), it can be regarded as one-dimensional, steady-state conduction with internal heat source:

$$T_{w,i}(x) = T_{w,o}(x) + \frac{q_v}{16k_{\text{steel}}}(D^2 - d^2) + \frac{q_v}{8k_{\text{steel}}}D^2 \ln \frac{d}{D} \quad (1)$$

Where  $T_{w,i}$  and  $T_{w,o}$  are the inner and outer wall temperatures of the tube, respectively.  $k_{\text{steel}}$  is the thermal conductivity of the tube.  $d$  and  $D$  are the inner and outer diameters of the tube. Since the thermal conductivity of the stainless steel tube varies with temperature and has a great impact on the data processing results, it should be calculated as

$$k_{\text{steel}} = 14.408(1 + 0.0011332T_w(x)) \quad (2)$$

$q_v$  is the heating power per unit volume of the tube and can be calculated as

$$q_v = \frac{IU}{[\pi(D^2 - d^2)L/4]} \quad (3)$$

Where  $L$  is the length of the heating section,  $U$  and  $I$  are the voltage and current of the tube.

The heating efficiency  $\eta$  of the test section can be calculated as

$$\eta = \frac{m(h_{\text{out}} - h_{\text{in}})}{UI} \quad (4)$$

Where  $h_{\text{out}}$  and  $h_{\text{in}}$  are the enthalpy of CO<sub>2</sub> at the inlet and outlet, respectively.  $m$  is the mass flow rate.  $h_{\text{out}}$  and

$h_{in}$  can be calculated from the temperature of inlet( $T_{in}$ ) and outlet( $T_{out}$ ) according to the following equation

$$\begin{aligned} h_{in} &= f(P, T_{in}) \\ h_{out} &= f(P, T_{out}) \end{aligned} \quad (5)$$

Heat flux  $q_w$  on the inner wall can be calculated as

$$q_w = \frac{\eta IU}{\pi dL} \quad (6)$$

The local bulk enthalpy of fluid  $h_b(x)$  can be calculated as

$$h_b(x) = h_{in} + (h_{out} - h_{in}) \times \frac{x}{L} \quad (7)$$

Where  $x$  represents the distance to the inlet.

The local bulk temperature of fluid  $T_b(x)$  can be calculated as

$$T_b(x) = f(P, h_b(x)) \quad (8)$$

The local heat transfer coefficient  $htc(x)$  is given by

$$htc(x) = \frac{q_w}{T_{w,i}(x) - T_b(x)} \quad (9)$$

### 2.3 Uncertainty analysis

The temperature at the inlet and outlet of the test section are measured by platinum resistance thermometers with uncertainty  $\pm 0.1^\circ\text{C}$ . The mass flow is measured using Endress+Hauser mass flow meter with uncertainty  $\pm 4\%$ . The pressure is measured by Rosemount pressure sensors with uncertainty  $\pm 0.1\%$ . Using Keysight direct current power (0~80V, 0~510A) for heating, the voltage and current uncertainties are  $\pm 0.1\%$  and  $\pm 0.2\%$ , respectively. The uncertainty of experimental parameters are calculated using the method by Moffat[10] in equation(10). The results are summarized in table 1.

$$\Delta y = \left[ \left( \frac{\partial y}{\partial x_1} \Delta x_1 \right)^2 + \left( \frac{\partial y}{\partial x_2} \Delta x_2 \right)^2 + \dots + \left( \frac{\partial y}{\partial x_n} \Delta x_n \right)^2 \right]^{1/2} \quad (10)$$

Table 1. Uncertainties of parameters

Parameters	Uncertainties	Parameters	Uncertainties
Bulk temperature	$\pm 0.1^\circ\text{C}$	Wall temperature	$\pm 0.2^\circ\text{C}$
Pressure	$\pm 0.1\%$	Mass flow	$\pm 0.4\%$
Voltage	$\pm 0.1\%$	Current	$\pm 0.2\%$
Heat flux	$\pm 4.3\%$	Heat transfer coefficient	$\pm 5.6\%$

### 2.4 Numerical method

Due to the supercritical fluid flows in a vertical circular tube and the heat flux is uniform, the flow field is axisymmetric, so it can be simplified to a two-dimensional(2D) axisymmetric model, which can significantly increase computational speed and reduce the calculation cost. The research results of many

scholars show that that the shear stress transport(SST)  $k-\omega$  turbulence model is the most accurate[6, 7]. So this model is also used in our work. More detailed information on the SST  $k-\omega$  turbulence model can be found in reference [11]. The physical properties of carbon dioxide are obtained from NIST Standard Reference Database 23 Version 9.0.

The model validation results are shown in figure 2, the results show that the simulation results are in good agreement with the experimental results, the wall temperature distribution trend of the simulated results is consistent with the experimental results. Although the temperature values are slightly different, the simulation results are only used for heat transfer mechanism analysis in this work, which is feasible.

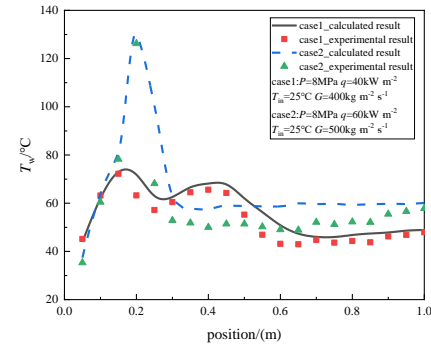


Fig. 2. Model verification results

## 3. RESULTS AND DISCUSSION

### 3.1 General characteristics and mechanism analysis

Figure 3 shows the experimental and simulation results at  $G=400 \text{ kg}\cdot\text{m}^{-2}\cdot\text{s}^{-1}$ ,  $q=40 \text{ kW}\cdot\text{m}^{-2}$ ,  $P=8 \text{ MPa}$ ,  $T_{in}=25^\circ\text{C}$ . The results show that local peaks appear in the wall temperature distribution. The wall temperature near the inlet suddenly increases sharply which indicate the deterioration of heat transfer. After reaching the peak, the wall temperature begins to show a downward trend, and then increases rapidly again. After the second peak, the wall temperature begins to decrease rapidly, and the heat transfer returns to normal, and then the wall temperature increases slowly.

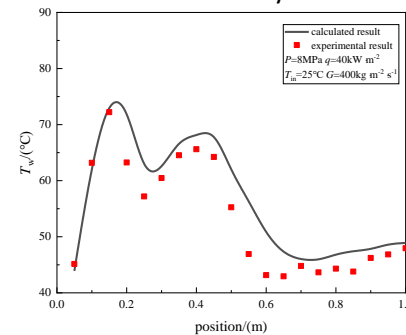


Fig. 3. Wall temperature results

In order to analyze the causes of peak wall temperature distribution and heat transfer deterioration, this paper conducts simulation under the same working conditions, and the results are shown in figure 3. The distributions of radial velocity and turbulent kinetic energy at different axial positions are obtained by simulation as shown in figure 4.

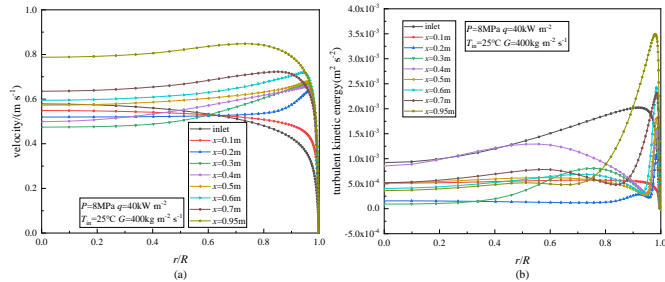


Fig. 4. Velocity(a) and turbulent kinetic energy(b) distributions at different axial positions

Results show that the turbulence develops fully and the U-shaped velocity profile is formed at the inlet, the value of velocity increases from the near wall region to the main flow region. At  $0.05\text{m}\sim 0.15\text{m}$ , as the fluid flows upward, the temperature of the fluid near the wall increases gradually and the density decreases rapidly. The density difference between the near wall and the main flow region causes strong buoyancy effect, which leads to velocity near the wall increases. So the velocity distribution near the wall is flattened as shown in figure 4(a), which causes the reduction of shear stress and turbulent kinetic energy as shown in figure 4(b). The turbulent diffusion of heat is impaired by the decrease of turbulent kinetic energy which makes the wall temperature increase rapidly. Thus, the strong buoyancy effect causes the peak of wall temperature and heat transfer deterioration.

At  $0.15\text{m}\sim 0.25\text{m}$ , with the fluid heating further, the fluid velocity near the wall continues to increase and exceeds that in the main flow region, forming an M-shaped velocity distribution, it results in a reverse shear stress. With the fluid flowing upward, the magnitude of shear stress and turbulent kinetic energy increases, which improves the turbulent diffusion of heat. Therefore, the wall temperature decreases gradually during this process.

At  $0.25\text{m}\sim 0.45\text{m}$ , in the main flow region, the temperature of the fluid increases gradually, the density decreases, and the velocity increases gradually which causes the velocity profile flattened again. Thus, the shear stress and turbulent kinetic energy decrease again, which causes the increase of wall temperature.

At  $0.45\text{m}\sim 0.7\text{m}$ , the fluid velocity in the main flow region increases continuously, the shear stress and

turbulent kinetic energy increase gradually, and the heat transfer return normal, so the wall temperature shows a downward trend. At  $0.7\text{m}\sim 1\text{m}$ , the fluid temperature exceeds the pseudo-critical temperature, the density varies slightly, so the buoyancy effect is almost negligible during this process. But the specific heat capacity decreases gradually with the increasing of temperature, so the wall temperature increases slowly.

### 3.2 Effects of mass flux

Figure 5 shows the variations of wall temperature ( $T_w$ ) and heat transfer coefficient ( $h_{tc}$ ) at different mass flux. The results show that the heat transfer deterioration occurs at low mass flux, wall temperature has obvious local peak while  $q/G \geq 0.1$  kJ/kg. The peak value of wall temperature decreases with the increasing of flux and the region of high temperature decreases gradually. It caused by the turbulence intensity increasing and the boundary layer decreasing with the mass flux increasing, heat from the wall can be transferred faster to the main area, and the buoyancy becomes weak. The effect of mass flux on heat transfer is particularly obvious while the bulk enthalpy is greater than 300 kJ/kg, the wall temperature is lower while the mass flux is larger at the same enthalpy. Because the specific heat of the fluid is larger at this time, the ability of the fluid to transport heat is stronger while the mass flux is larger. Moreover, the buoyancy effect becomes weaker with the increasing of mass flux.

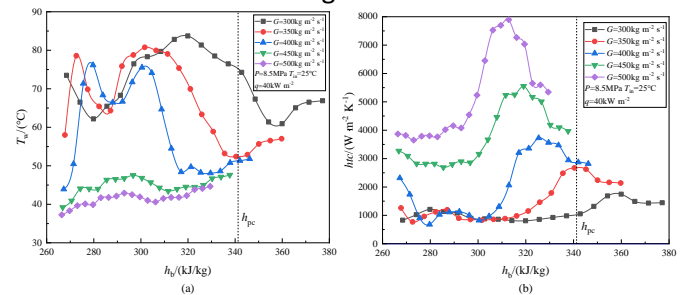


Fig. 5. Effect of mass flux on heat transfer. (a).  $T_w$  (b).  $h_{tc}$

### 3.3 Effects of heat flux

Figure 6 shows the variations of wall temperature and heat transfer coefficient at different heat flux. The results show that the heat transfer deterioration occurs at high heat flux, wall temperature has obvious local peak while  $q/G \geq 0.1$  kJ/kg. The peak value of wall temperature decreases with the decreasing of heat flux and the region of high temperature decreases gradually. The heat transfer coefficient decreases with the increasing of heat flux, and because of the heat transfer deterioration, the heat transfer coefficient shows obvious valley near the inlet as shown in figure 6(b). The

heat transfer coefficient begins to increase after passing the deterioration region as the increasing of the specific heat capacity.

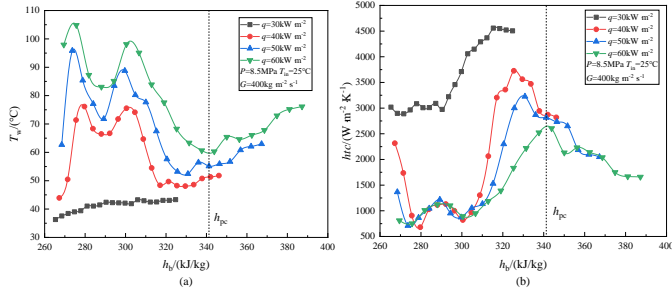


Fig. 6. Effect of heat flux on heat transfer. (a).  $T_w$  (b).  $htc$

### 3.4 Effects of pressure

The variations of wall temperature and heat transfer coefficient under different pressures are shown in figure 7. The results show that the wall temperature and heat transfer coefficient are slightly affected by pressure in the low enthalpy region. Because the temperature of the fluid is low and away from the pseudo-critical region, the physical properties of fluid vary little at different pressures, the performance of heat transfer is similar.

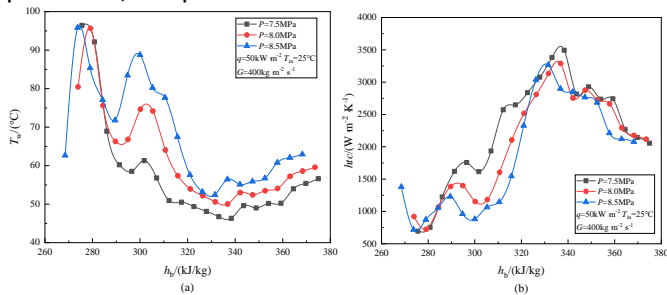


Fig. 7. Effect of pressure on heat transfer. (a).  $T_w$  (b).  $htc$

The wall temperature and heat transfer coefficient are significantly different under various pressures while the enthalpy of the fluid reaches 300kJ/kg. Because the state of the fluid is close to the pseudo-critical region, the physical properties of the fluid are greatly affected by the pressure, especially the specific heat capacity. The heat transfer performance at low pressure is better than that at high pressure. As the temperature of the fluid increases further and exceeds the pseudo-critical temperature, the difference in heat transfer performance begins to diminish. Thus, the heat transfer performance is greatly affected by the pressure near the pseudo-critical region, but the effect is slight while far from the pseudo-critical region.

### 3.5 Effects of inlet temperature

Figure 8 shows the variation of wall temperature and heat transfer coefficient at different inlet temperatures. The results show that the change in inlet temperature has little effect on the distribution of wall temperature

and heat transfer coefficient under the same working condition. For the wall temperature, the local peak still exists. For the heat transfer coefficient, the peak appears while the fluid temperature near pseudo-critical temperature under all these conditions. The peak value of heat transfer coefficient increases slightly with the increasing of inlet temperature. In the section near the inlet, the fluid temperature is far away from the pseudo-critical temperature, the physical properties of the fluid have little difference at different temperatures, so the inlet temperature has little influence on the heat transfer coefficient near the inlet. However, the fluid temperature gradually increases and approaches the pseudo-critical temperature as the fluid is heated. The effect of temperature on physical properties is obvious, so the heat transfer coefficient in the latter part of the test section is slightly different. In general, the inlet temperature has little effect on the heat transfer performance.

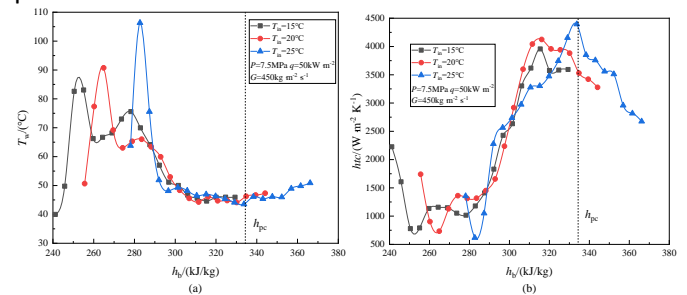


Fig. 8. Effect of inlet temperature on heat transfer. (a).  $T_w$  (b).  $htc$

## 4. HEAT TRANSFER CORRELATION

The experimental results show that the variations in thermophysical properties and the buoyancy effect have a significant effect on heat transfer. Therefore, the difference in specific heat capacity and thermal conductivity between the wall and the main flow area must be taken into account in proposing the heat transfer correlation. Since the difference in density between the wall and the main flow area leads to the buoyancy effect, the density difference is also taken into account. Based on 535 experimental data points, the heat transfer correlation is proposed by multiple linear regression as follow

$$Nu_b = 0.01454 R e_b^{0.8569} P r_b^{1.1901} \left( \frac{c_{p,w}}{c_{p,b}} \right)^{0.9458} \left( \frac{\rho_w}{\rho_b} \right)^{0.4282} \left( \frac{\lambda_w}{\lambda_b} \right)^{0.3403} \quad (11)$$

Figure 9 is a comparison between the data calculated by the heat transfer correlation equation and the experimental data. It can be seen from the figure that the deviation between the experimental data and the calculated data is no more than  $\pm 25\%$ , indicating that the obtained heat transfer correlation equation can better

predict the Nu number in the mainstream area while S-CO<sub>2</sub> flows vertically upward in the heating tube.

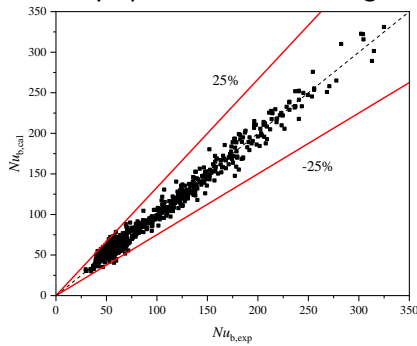


Fig. 9. The comparison between the simulated Nu and calculated Nu by the correlation

## 5. CONCLUSION

The heat transfer characteristics of S-CO<sub>2</sub> flowing upward in a vertical tube ( $d=4.57\text{mm}$ ) is studied in this paper by experimental and numerical method. The main conclusions of this paper are summarized as follows:

(1) The simulation results show that the velocity distribution is flattened due to the buoyancy effect caused by the large density difference between the near wall and the main flow in the pseudo-critical region. So the shear stress and turbulent kinetic energy decrease which impairs the turbulent diffusion of heat and heat transfer deterioration occurs.

(2) The experimental results show that heat transfer deterioration occurs while  $q/G \geq 0.1\text{kJ/kg}$ . The heat transfer performance is better at higher mass flux or lower heat flux. Pressure and inlet temperature affect heat transfer only while the fluid state is near the pseudo-critical region.

(3) Based on 535 experimental data points, a heat transfer correlation is proposed with the largest prediction deviation of less than 25% which can be applied in the design of S-CO<sub>2</sub> Brayton cycle system.

## ACKNOWLEDGEMENT

The authors gratefully acknowledge the National Natural Science Foundation of China for the financial support (Grant No. 51876198, 52006211). The numerical calculations have been done on the supercomputing system in the Supercomputing Center of University of Science and Technology of China.

## REFERENCE

- [1] J. Xu, C. Liu, E. Sun, J. Xie, M. Li, Y. Yang, et al. Perspective of S-CO<sub>2</sub> power cycles. *Energy*. 186 (2019).
- [2] L. Chai, S.A. Tassou. A review of printed circuit heat exchangers for helium and supercritical CO<sub>2</sub> Brayton

cycles. *Thermal Science and Engineering Progress*. 18 (2020).

[3] M. Ding, J. Liu, W.-L. Cheng, W.-X. Huang, Q.-N. Liu, L. Yang, et al. An adaptive flow path regenerator used in supercritical carbon dioxide Brayton cycle. *Applied Thermal Engineering*. 138 (2018) 513-22.

[4] J.-W. Zhao, R. Zhao, Y.-L. Nian, W.-L. Cheng. Experimental study of supercritical CO<sub>2</sub> in a vertical adaptive flow path heat exchanger. *Applied Thermal Engineering*. 188 (2021).

[5] S. Zhang, X. Xu, C. Liu, X. Liu, C. Dang. Experimental investigation on the heat transfer characteristics of supercritical CO<sub>2</sub> at various mass flow rates in heated vertical-flow tube. *Applied Thermal Engineering*. 157 (2019).

[6] X. Lei, J. Zhang, L. Gou, Q. Zhang, H. Li. Experimental study on convection heat transfer of supercritical CO<sub>2</sub> in small upward channels. *Energy*. 176 (2019) 119-30.

[7] S. Yildiz, D.C. Groeneveld. Diameter effect on supercritical heat transfer. *International Communications in Heat and Mass Transfer*. 54 (2014) 27-32.

[8] S. Zhang, X. Xu, C. Liu, X. Liu, Z. Ru, C. Dang. Experimental and numerical comparison of the heat transfer behaviors and buoyancy effects of supercritical CO<sub>2</sub> in various heating tubes. *International Journal of Heat and Mass Transfer*. 149 (2020).

[9] J. Guo, M. Xiang, H. Zhang, X. Huai, K. Cheng, X. Cui. Thermal-hydraulic characteristics of supercritical pressure CO<sub>2</sub> in vertical tubes under cooling and heating conditions. *Energy*. 170 (2019) 1067-81.

[10] R.J. Moffat. Describing the uncertainties in experimental results. *Exp Therm Fluid Sci*. 1 (1988).

[11] ANSYS Inc. ANSYS fluent theory guide release 15.0. 2013.